Available online at www.sciencedirect.com
ScienceDirect
Ceramics International 35 (2009) 453–456
CERAMICS INTERNATIONAL
www.elsevier.com/locate/ceramint

High-pressure sintered yttria stabilized zirconia ceramics

Q. Li [a,b], Y.F. Zhang [a,b], X.F. Ma [a], J. Meng [a], X.Q. Cao [a,*]

[a] *Key Lab of Rare Earth Chemistry and Physics, Changchun Institute of Applied Chemistry, Chinese Academy of Sciences, Changchun 130022, Jilin, China*
[b] *Graduate School of Chinese Academy of Sciences, Beijing 100049, China*

Received 24 May 2007; received in revised form 29 August 2007; accepted 6 December 2007
Available online 8 April 2008

Abstract

Fast densification of 8YSZ ceramics under a high pressure of 4.5 GPa was carried out at different temperatures (800, 1000, 1450 °C), by which a high relative density above 92% could be obtained. FT-Raman spectra indicate that the 8YSZ underwent a phase transition from partially tetragonal to partially cubic phase as temperatures increase from 1000 to 1450 °C when sintering under high pressure. The electrical properties of the samples under different high-pressure sintering conditions were measured by complex impedance method. The total conductivity of 0.92×10^{-2} S cm^{-1} at 800 °C has been obtained for 8YSZ under high pressure at 1450 °C, which is about 200 °C lower than that of the samples prepared by conventional pressureless sintering.

Keywords: A. Sintering; C. Electrical conductivity; Microstructure; Yttria stabilized zirconia

1. Introduction

8 mol% yttria stabilized zirconia (8YSZ) is a common solid oxide electrolyte because of its good ionic conductivity at temperature above 800 °C. However, without sintering, it is difficult to be fully sintered at comparatively low temperatures. The sintering at high temperatures may lead to many problems such as the energy cost, degradation of the quality of the materials, excessive grain growth and unfavorable interface reaction between ZrO_2-based materials and other components. Therefore, low temperature processing of dense YSZ ceramics is of practical significance as it provides better mechanical properties of the electrolytes, energy saving, and most importantly the possible co-firing of YSZ electrolytes with other SOFCs components. Up to now, many studies have been carried out on the low temperature consolidation of the nanomaterials [1–5]. For electrolyte materials, dense and fine-grained $La_2Mo_2O_9$ ceramic has been prepared by a novel three-stage thermal processing method [6] and spark plasma sintering method [7]. CeO_2-based ceramic electrolytes have been obtained at low temperature by spark plasma sintering method [8]. The above studies have an improvement of electrical properties.

Due to the technical importance of ZrO_2-based ceramics, plenty of efforts have also been made to the development of sintering methods during recent years. Dahl et al. [9] studied densification and properties of zirconia prepared by hot pressing, spark plasma sintering and conventional sintering methods. Although no significant differences in electrical conductivity were observed for ZrO_2-based materials by the different sintering methods, it reduced sintering temperature and time, which is helpful for facilitating co-firing electrolytes with other SOFCs components, especially for improving the performance of SOFCs.

Besides hot pressing and spark plasma sintering, high-pressure sintering is an effective method to fabricate the dense nanoceramics. In this process, a high pressure is applied on the sample during heating, giving rise to reduction of the sintering temperature and duration, and the fine microstructures was obtained. The study on fabrication of nano Y-TZP materials by superhigh-pressure compaction has been reported in the literature [10]. In the present work, the microstructure, phase stability of the 8YSZ ceramics as a function of sintering temperature by high-pressure densification are studied.

* Corresponding author. Tel.: +86 431 85262285; fax: +86 431 85262285.
E-mail address: xcao@ciac.jl.cn (X.Q. Cao).

0272-8842/$34.00
doi:10.1016/j.ceramint.2007.12.002

2. Experimental

Powders of nanocrystalline 8YSZ were synthesized by a sol–gel method. $ZrOCl_2{\cdot}8H_2O$ and Y_2O_3 were selected as precursors. Y_2O_3 was dissolved into a hot nitric acid to obtain yttrium nitrate solution, and $ZrOCl_2{\cdot}8H_2O$ were dissolved into the deionized water. These two solutions in a stoichiometric ratio were then mixed and stirred continuously until a homogenous solution was obtained. Citric acid and ethylene glycol were then added and stirred at 70 °C till gellation was completed. Then the gel was dried at 110 °C and calcined at different temperatures.

Compaction was completed using a cubic-type high-pressure equipment with six WC anvils (DS-029C, China). The powder was firstly compacted at 200 MPa, and then the green compact was loaded in a graphite sleeve heater, encapsulated in a cube die made of pyrophyllite, and then the residual room was filled with h-BN as heat-transmitting medium. High mechanical pressure was then applied. In this way, the samples were sintered under a high pressure of 4.5 GPa at different temperatures for a very short time.

An environmental scanning electron microscope (Philips, XL30) was used to investigate the morphology of the prepared samples. FT Raman spectra were recorded on a Thermal Nicolet FT-Raman 960 equipped with an InGaAs detector and the incident power was 300 mW. AC impedance study was carried out on pellets. Electrodes were made by coating the both sides of the pellet with platinum paste followed by heating up to 800 °C at a rate of 10 °C min^{-1} and dwelling for 1 h. Impedance data were collected on a Solartron SI 1255 High Frequency Response Analyzer coupled with a SI 1287 Electrochemical Interface over the frequency range of 1 MHz to 0.1 Hz with an applied voltage of 10 mV.

3. Results and discussion

3.1. Characterization of powders

The X-ray diffraction (XRD) patterns of nanopowder calcined at different temperatures with the sol–gel method are shown in Fig. 1. The line broadening in the X-ray diffraction peaks at 600 °C indicates the formation of nanocrystals. With the increase of the calcinations temperature, the XRD peaks get sharper, implying that the grain size was increased. For the sample calcined at 600 °C, the grain size was estimated to be about 20 nm according to Scherrer's equation

$$d = \frac{0.90\lambda}{\beta \cos\theta} \quad (1)$$

where β is the calibrated full width at half maximum of the peak and θ is the diffraction angle [11], and the result was confirmed by the SEM photo in the insert of Fig. 1.

3.2. Microstructure

The nanopowders calcinated at 600 °C were firstly pressed into cylindrical pellets under 200 MPa, and then sintered into pellets under a high pressure of 4.5 GPa at different temperatures for a short time. Fig. 2 shows the XRD patterns of the as-sintered pellets. It can be seen that extra peaks appeared for the as-sintered samples at 800 °C for 5 and 10 min, which can be indexed with BN contamination of the surface. When sintering temperature was increased to 1000 °C, no extra peaks were observed. The peaks were still broadened due to the nano-effect. Fig. 3 shows the SEM photos of the samples sintered under high pressure at different temperatures. The grain size is about 28 nm for the sample sintered at 1000 °C, which is consistent with the calculation results of Scherrer's equation. When the temperature was increased to 1450 °C, the grain growth was serious and reaches 0.5–1 μm as shown in Fig. 3b. It is, therefore, concluded that the temperature is one of the key factors to influence the grain growth in the sintering process. The low sintering temperature prevents the excessive grain growth during the sintering, which is critical for obtaining nanocrystalline ceramics. Relative density and grain size of the ceramics sintered at different temperatures are shown in Table 1. For the sample densified at 800 °C, the density is 5.48 g cm^{-3}, which is 92% of the theoretical value. As the sintering temperature was increased, the density of the sample increased slightly.

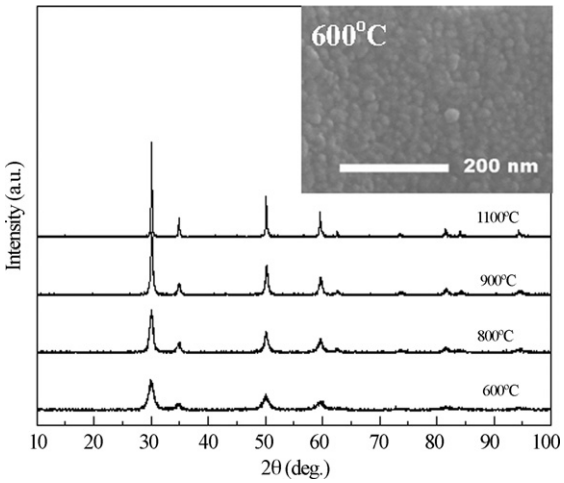

Fig. 1. XRD patterns of 8YSZ nanopowders calcinated at different temperatures for 10 h, and the insert is the SEM photo of 8YSZ nanopowder calcined at 600 °C.

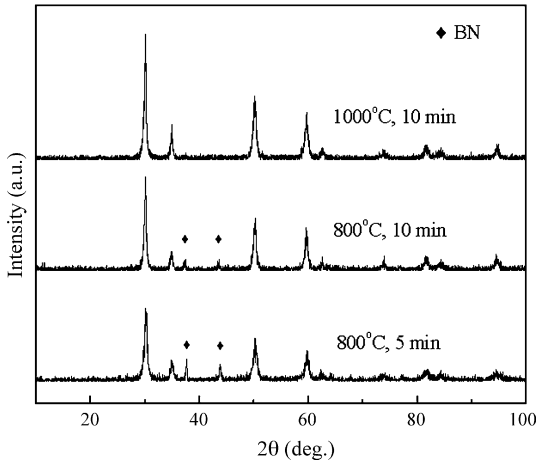

Fig. 2. XRD patterns of 8YSZ sintered under 4.5 GPa at different temperatures.

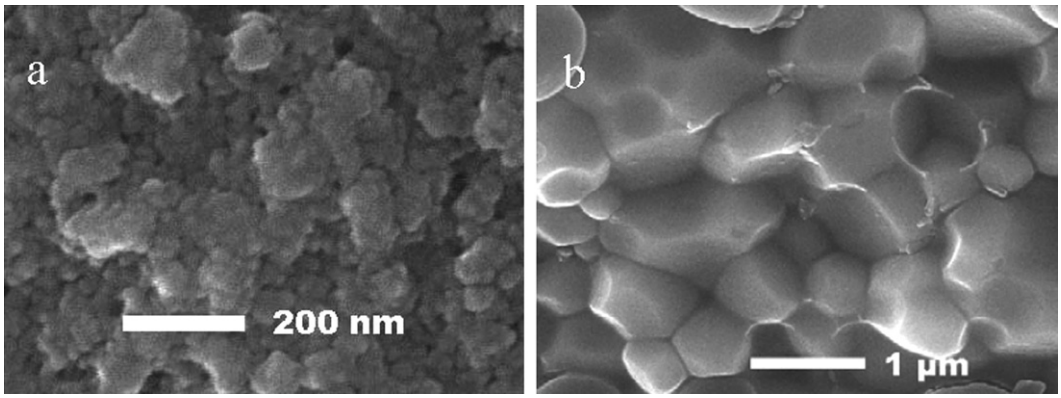

Fig. 3. SEM photos of 8YSZ sintered under 4.5 GPa at 1000 °C (a) and 1450 °C (b) for 10 min.

Table 1
Characterization of 8YSZ prepared by different methods

Samples	Temperature (°C)	Dwelling time (min)	Grain size	Relative density (%)
8YSZ	800	10	~23 nm	~92
	1000	10	~28 nm	92
	1450	10	0.5–1 μm	94

3.3. Phase composition

Raman spectroscopy is considered to be a powerful tool to provide the information on zirconia [12]. Fig. 4 exhibits the FT Raman spectra of the 8YSZ samples sintered at different temperatures. The FT Raman spectra of high-pressure sintered 8YSZ at 1000 °C have been studied before [13]. It can be indexed in tetragonal and monoclinic phase. Herein, the FT Raman spectra of high-pressure sintered 8YSZ at 1450 °C have been given for comparison. In the case of the sample sintered at 1450 °C, the peaks are found to be different from that of the sample sintered at 1000 °C. The strong peak at 630 cm^{-1} and additional weak features at 240 and 150 cm^{-1} indicate that the cubic phase is present [14], while the bands at 377 and 470 cm^{-1} indicate the existence of traces of the monoclinic and tetragonal phase [15]. In summary, the 8YSZ underwent a phase transition from partially tetragonal to partially stabilized cubic phase as temperatures increase from 1000 to 1450 °C when sintering under high pressure.

3.4. Electrical conductivity

Ac complex spectra were used to analyze the electrical properties of the samples. Fig. 5 presents the typical complex spectra of samples sintered under high pressure at 1450 °C measured at 400 °C. The nonlinear curve fitting of these impedance data was carried out by software Zview using a circuit model as seen in the insert in Fig. 4. The values of capacitive obtained from the circuit model are 829 PF and 4.91 μF, respectively. The total resistance can be obtained from the impedance spectra according to

$$R_{total} = R_b + R_{gb} \quad (2)$$

and then converted to a conductivity σ, using the relation

$$\sigma = \frac{L}{SR} \quad (3)$$

where L is the sample thickness; and S, the electrode area on the sample surface. The total conductivity of the samples as

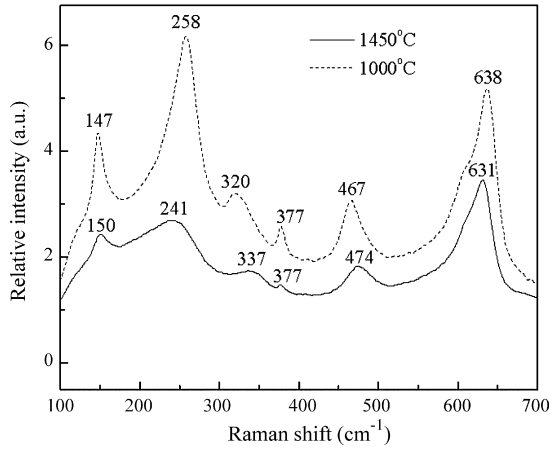

Fig. 4. FT-Raman spectra of 8YSZ sintered under 4.5 GPa at different temperatures for 10 min.

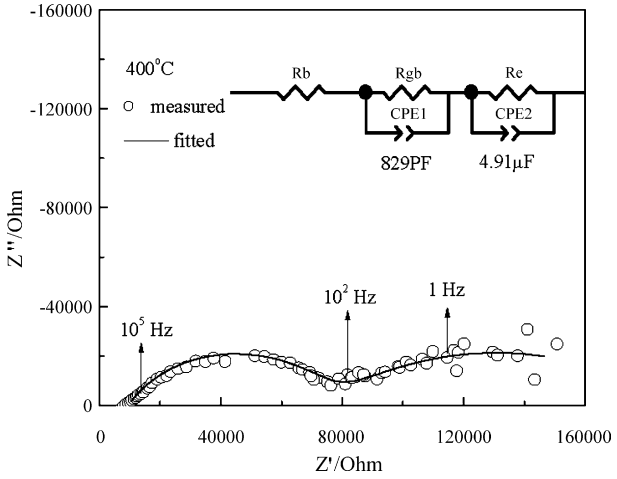

Fig. 5. AC impedance spectra at 400 °C for 8YSZ sintered under 4.5 GPa at 1450 °C for 10 min.

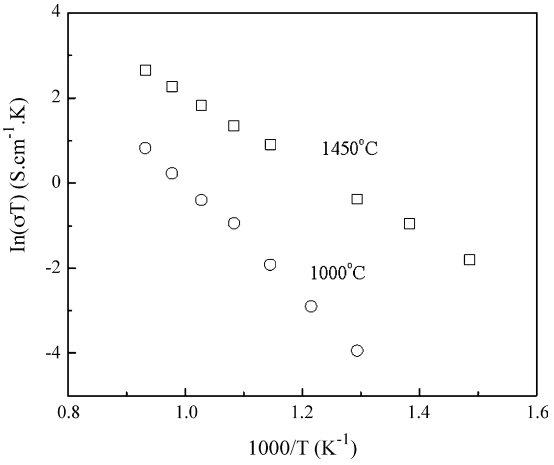

Fig. 6. Electrical conductivities of 8YSZ sintered under 4.5 GPa at different temperatures for 10 min.

function of temperature is shown in the form of Arrhenius plots in Fig. 6. It can be seen that sample sintered under high pressure at 1450 °C has *a* higher electrical conductivity than the one of sample sintered under high pressure at 1000 °C. The total conductivity of 8YSZ sintered under high pressure at 1450 °C is 0.92×10^{-2} S cm^{-1} at 800 °C. Compared with the 8YSZ by traditional pressureless sintering, the 8YSZ by high-pressure sintering at 1450 °C gained approximately full density and an identical electrical property. In addition, by pressureless sintering, it is important to underline that this sintering temperature is 1650 °C for density lower than 90% in our work. The use of high-pressure sintering method allows a decrease of more than 200 °C of the sintering temperature.

4. Conclusion

Nanocrystalline 8YSZ powders prepared by sol–gel methods were sintered under a high pressure of 4.5 GPa at different temperatures. FT Raman spectra indicate that the 8YSZ underwent a phase transition from partially tetragonal to partially cubic phase as temperatures increased from 1000 to 1450 °C when sintering under high pressure. Electrical measurements indicate that the high-pressured sample at 1450 °C has the same electrical conductivity as that of sample prepared by traditional pressureless sintering. The low sintering temperature 1450 °C achieved in the present work is of practical significance for maintaining the cubic phase and facilitating co-firing the 8YSZ electrolytes with other SOFCs components.

Acknowledgement

This work was financially supported by A1320061002.

References

[1] Y.S. Zhang, L.T. Hu, J.M. Chen, W.M. Liu, Preparation of Y-TZP Nanoceramics by gelcasting-pressing method and pressureless sintering, Adv. Eng. Mater. 8 (4) (2006) 271–275.
[2] J.G. Li, T. Ikegami, T. Mori, Low temperature processing of dense samarium-doped CeO_2 ceramics: sintering and grain growth behaviors, Acta Mater. 52 (8) (2004) 2221–2228.
[3] Z. Lei, Q.S. Zhu, Low temperature processing of dense nanocrystalline scandia-doped zirconia (ScSZ) ceramics, Solid State Ion. 176 (37–38) (2006) 2791–2797.
[4] U.A. Tamburini, J.E. Garay, Z.A. Munir, Fast low-temperature consolidation of bulk nanometric ceramic materials, Scr. Mater. 54 (5) (2006) 823–828.
[5] K.A. Khor, L.-G. Yu, S.H. Chan, X.J. Chen, Densification of plasma sprayed YSZ electrolytes by spark plasma sintering (SPS), J. Eur. Ceram. Soc. 23 (11) (2003) 1855–1863.
[6] J.X. Wang, X.P. Wang, F.J. Liang, Z.J. Cheng, Q.F. Fang, Enhancement of conductivity in $La_2Mo_2O_9$ ceramics fabricated by a novel three-stage thermal processing method, Solid State Ion. 177 (17–18) (2006) 1437–1442.
[7] J.H. Yang, Z.Y. Wen, Z.H. Gu, D.S. Yan, Ionic conductivity and microstructure of solid electrolyte $La_2Mo_2O_9$ prepared by spark-plasma sintering, J. Eur. Ceram. Soc. 25 (14) (2005) 3315–3321.
[8] M.G. Bellino, D.G. Lamas, N.E. Walsöe de Reca, Enhanced ionic conductivity in nanostructured, heavily doped ceria ceramics, Adv. Func. Mater. 16 (1) (2006) 107–113.
[9] P. Dahl, I. Kaus, Z. Zhao, M. Johnsson, M. Nygren, K. Wiik, T. Grande, M.-A. Einarsrud, Densification and properties of zirconia prepared by three different sintering techniques, Ceram. Inter. 33 (8) (2007) 1603–1610.
[10] L. Gao, W. Li, H.Z. Wang, J.X. Zhou, Z.J. Chao, Q.Z. Zai, Fabrication of nano Y–TZP materials by superhigh pressure compaction, J. Eur. Ceram. Soc. 21 (2) (2001) 135–138.
[11] K.K. Ral, T. Banu, M. Vithal, G.Y.S.K. Swamy, K.R. Kumar, Preparation and characterization of bulk and nano particles of $La_2Zr_2O_7$ and $Nd_2Zr_2O_7$ by sol–gel method, Mater. Lett. 54 (2–3) (2002) 205–210.
[12] G. Xu, Y.W. Zhang, C.S. Liao, C.H. Yan, Doping and grain size effects in nanocrystalline ZrO_2–Sc_2O_3 system with complex phase transitions: XRD and Raman studies, Phys. Chem. Chem. Phys. 6 (23) (2004) 5410–5418.
[13] Q. Li, T. Xia, X.D. Liu, X.F. Ma, J. Meng, X.Q. Cao, Fast densification and electrical conductivity of yttria-stabilized zirconia nanoceramics, Mater. Sci. Eng. B 138 (1) (2007) 78–83.
[14] C.M. Phillippi, K.S. Mazdiyasni, Infrared and Raman spectra of zirconia polymorphs, J. Am. Ceram. Soc. 54 (5) (1971) 254–258.
[15] M.J. Li, Z.C. Feng, G. Xiong, P.L. Ying, Q. Xin, C. Li, Phase transformation in the surface region of zirconia detected by UV Raman spectroscopy, J. Phys. Chem. B 105 (34) (2001) 8107–8111.